Landscape and climatic variations of the Quaternary shaped multiple secondary contacts among barn owls (*Tyto alba*) of the Western Palearctic

Tristan Cumer[1*], Ana Paula Machado[1], Guillaume Dumont [1], Vasileios Bontzorlos[2,3], Renato Ceccherelli[4,] Motti Charter[5,6], Klaus Dichmann[7], Hans-Dieter Martens[8], Nicolaos Kassinis[9], Rui Lourenço[10], Francesca Manzia[11], Laure Prévost[12], Marko Rakovic[13], Felipe Siverio[14], Alexandre Roulin[‡1], Jérôme Goudet[‡1,15]

‡ co-senior authors
* corresponding author

Contact details for corresponding author: Department of Ecology and Evolution, Biophore 13 Building, University of Lausanne, CH -1015 Lausanne, Switzerland. Tel: +41 21 692 42 18. Email: Tristan.cumer@unil.ch

1 Department of Ecology and Evolution, University of Lausanne, Lausanne, Switzerland
2 Green Fund, Kifisia, Athens, Greece
3 "TYTO" - Organization for the Management and Conservation of Biodiversity in Agricultural Ecosystems, Larisa, Greece
4 Centro Recupero Rapaci del Mugello, Firenze, Italy
5 Shamir Research Institute, University of Haifa, Katzrin, Israel
6 Department of Geography and Environmental Sciences, University of Haifa, Haifa, Israel
7 Hyldehegnet 27, 6400 Sønderborg, Denmark
8 Gettorfer Weg 13, 24214 Neuwittenbek, Germany
9 Game and Fauna Service, Ministry of the Interior, Nicosia, Cyprus
10 MED Mediterranean Institute for Agriculture, Environment and Development, Laboratory of Ornithology, IIFA, University of Évora, Évora, Portugal
11 Centro di Recupero per la Fauna Selvatica–LIPU, Rome, Italy
12 Association C.H.E.N.E., Centre d'Hébergement et d'Etude sur la Nature et l'Environnement, 76190 Allouville-Bellefosse, France
13 Natural History Museum of Belgrade, Belgrade, Serbia
14 Canary Islands' Ornithology and Natural History Group (GOHNIC) 38480 Buenavista del Norte, Tenerife, Canary Islands, Spain
15 Swiss Institute of Bioinformatics, Lausanne, Switzerland

Tristan Cumer - 0000-0002-0276-7462
Ana Paula Machado - 0000-0001-9203-7000
Motti Charter - 0000-0003-3861-6356
Nicolaos Kassinis - 0000-0003-2559-6683
Rui Lourenço - 0000-0001-7694-0478
Marko Rakovic - 0000-0002-3658-3362
Felipe Siverio - 0000-0002-0324-0646
Alexandre Roulin - 0000-0003-1940-6927
Jérôme Goudet - 0000-0002-5318-7601

47 Key words
48
49 Demographic modeling; glacial refugium; Haplotypes; Population genomics; postglacial
50 recolonization; Whole-genome resequencing

Abstract

The combined actions of climatic variations and landscape barriers shape the history of natural populations. When organisms follow their shifting niches, obstacles in the landscape can lead to the splitting of populations, on which evolution will then act independently. When two such populations are reunited, secondary contact occurs in a broad range of admixture patterns, from narrow hybrid zones to the complete dissolution of lineages. A previous study suggested that barn owls colonized the Western Palearctic after the last glaciation in a ring-like fashion around the Mediterranean Sea, and conjectured an admixture zone in the Balkans. Here, we take advantage of whole-genome sequences of 94 individuals across the Western Palearctic to reveal the complex history of the species in the region using observational and modeling approaches. Even though our results confirm that two distinct lineages colonized the region, one in Europe and one in the Levant, they suggest that it predates the last glaciation and identify a narrow secondary contact zone between the two in Anatolia. Nonetheless, we also show that barn owls re-colonized Europe after the glaciation from two distinct glacial refugia: a western one in Iberia and an eastern one in Italy. Both glacial lineages now communicate via eastern Europe, in a wide and permeable contact zone. This complex history of populations enlightens the taxonomy of *Tyto alba* in the region, highlights the key role played by mountain ranges and large water bodies as barriers and illustrates the power of population genomics in uncovering intricate demographic patterns.

Introduction

Species distribution patterns fluctuate in response to climatic variations, as populations relocate to follow their shifting niches[1]. When organisms colonize new areas, obstacles in the landscape may lead populations to split with varying degrees of geographic isolation. Evolution, via mutation, drift, local adaptation and gene flow, will then act independently on each of the isolated populations. If two allopatric populations are later geographically reconnected, after a certain amount of time and divergence, it can create a secondary contact zone. For example, when populations on both sides of an obstacle meet at the end of it in a ring-like fashion, as described in birds [2], amphibiens [3, 4], or plants [5]. Likewise, climate oscillations can lead to cyclical isolation and secondary contacts between populations as regional suitability varies [6].

This complex interplay between climatic variations and landscape has been extensively studied in the Western Palearctic [7,8], specifically in light of the cycles of glacial and interglacial periods that characterized the Quaternary [9]. During the last glaciation, colder temperatures and the expansion of the ice sheets in the north rendered large areas unsuitable for many species, which led them to follow their niches southward. Species found refuge in the Mediterranean peninsulas and in northern Africa where climatic conditions were more amenable, forming isolated populations. At the end of the last glaciation maximum (i.e. approximatively 20k years ago [10]), this process was reversed as the climate warmed and the melting of the continental ice caps exposed free land that could be recolonized. An extensive literature addressing the post-glacial history of European organisms describes how the complex landscape of the continent, combined with the distribution of species during the glaciation, conditioned their recolonization processes [8,11]. However, the low-resolution of

93 genetic data used before the genomic era was often insufficient to resolve the intricate and
94 often fine-scale evolutionary processes that occurred during recolonization.
95 Rapid development of high-throughput sequencing technologies and corresponding
96 methodological tools during the last decades has opened new avenues to study natural
97 populations with high precision. In particular, it has allowed biologists to reconstruct the
98 evolutionary history of species and highlight the diversity of processes acting when
99 populations or subspecies interact in secondary contact. These processes have been found to
100 result in a variety of situations. While the prolonged isolation of populations may lead to
101 allopatric speciation (many examples in plants [12,13], amphibian [3], insects [14], mammals [15] and
102 birds [16]), secondary contact tends to show a broad range of admixture patterns. When
103 admixture occurs, it may vary from narrow hybrid zones between lineages [17], to the complete
104 dissolution of a lineage [18], through a gradual level of admixture along a gradient of mixing
105 populations [19].
106 Microsatellite and mitochondrial data suggested that the barn owls (*Tyto alba*), a non-
107 migratory raptor, colonized the Western Palearctic in a ring-like fashion around the
108 Mediterranean Sea after the last glaciation [20]. Under this scenario, a postglacial expansion
109 from the glacial refugium in the Iberian Peninsula to northern Europe formed the western
110 branch of the ring, with the eastern branch present across the Levant and Anatolia. While
111 these observations led to conjecture of a potential admixture zone in the Balkans, the
112 available data at the time combined with the overall low genetic differentiation in this species
113 did not allow to fully resolve this question. Moreover, the peculiar genetic makeup of
114 populations in the presumed contact zone brought into question the possibility of a cryptic
115 glacial refugium in the eastern Mediterranean peninsulas.

116 The difficulty in resolving the post glacial expansion of barn owls is mirrored by their
117 convoluted taxonomy in the Western Palearctic. In this region, *Tyto alba* is classified into
118 different subspecies based on geography and plumage coloration. First, *T. a. erlangeri*
119 (Sclater, WL, 1921) reported in Crete, Cyprus and Middle East, may match the Levant lineage.
120 Second, *T. a. alba* (Scopoli, 1769) is white-colored and supposedly present in western Europe
121 and western Canary Islands, and could represent the western arm of the ring colonization. *T.*
122 *a. guttata* (Brehm, CL, 1831), the third subspecies is a dark rufous morph allegedly found in
123 Northern and Eastern Europe, in the Balkans and around the Aegean Sea. This taxonomy does
124 not match any known genetic lineage identified so far and overlaps with the area where
125 admixture between the two lineages that colonized Europe supposedly happens, making the
126 presence of a subspecies in this area puzzling in light of the history known so far.
127 Here, taking advantage of whole genome sequences of 94 individuals from all around
128 continental Europe and the Mediterranean Sea, we elucidate the demographic history of barn
129 owls in the Western Palearctic. Combining descriptive and modelling approaches based on
130 genomic and ecological data, we identify how the climatic variations and landscape of the
131 region shaped the history of this species. We also investigate how previously isolated
132 populations of barn owls interact at secondary contacts between different lineages, and
133 discuss the convoluted taxonomy with regards to their history.

Material and methods

Samples and data preparation

Sampling, molecular and sequencing methods

The whole genomes of 96 individual barn owls (*Tyto alba*) were used in this study (table S1): 94 individuals were sampled in 11 Western Palearctic localities: Canary Islands (Tenerife island - WC), Portugal (PT), France (FR), Switzerland (CH), Denmark (DK), Serbia (SB), Greece (GR), Italy (IT), Aegean islands (AE), Cyprus (CY) and Israel (IS). In addition, one Eastern (*Tyto javanica* from Singapore) and one American barn owl (*Tyto furcata* from California, USA) were used as outgroups. Illumina whole-genome sequences of individuals from PT, FR, CH, DK and the outgroups were obtained from the GenBank repository (BioProject PRJNA700797). For the remaining 61 individuals, we followed a similar library preparation and sequencing protocol as outlined in Machado et al. [21]. Briefly, genomic DNA was extracted using the DNeasy Blood & Tissue kit (Qiagen, Hilden, Germany), and individually tagged. 100bp TruSeq DNA PCR-free libraries (Illumina) were prepared according to manufacturer's instructions. Whole-genome resequencing was performed on multiplexed libraries with Illumina HiSeq 2500 PE high-throughput sequencing at the Lausanne Genomic Technologies Facility (GTF, University of Lausanne, Switzerland).

Data processing, SNP calling and technical filtering

The bioinformatics pipeline used to obtain analysis-ready SNPs was adapted from the Genome Analysis Toolkit (GATK) Best Practices [22] to a non-model organism following the developers' instructions, as in Machado et al. [21]. Raw reads were trimmed with Trimommatic v.0.36 [23] and aligned to the reference barn owl genome [21] with BWA-MEM v.0.7.15 [24]. Base

158 quality score recalibration (BQSR) was performed using high-confidence calls obtained from
159 two independent callers – GATK's HaplotypeCaller and GenotypeGVCF v.4.1.3 and ANGSD
160 v.0.921 [25] – as a set of "true variants" in GATK v.4.1.3.
161 Genotype calls were filtered for analyses using a hard-filtering approach as proposed for non-
162 model organisms, using GATK and VCFtools [26]. Calls were removed if they presented: low
163 individual quality per depth (QD < 5), extreme coverage (1100 > DP > 2500), mapping quality
164 (MQ < 40 and MQ > 70), extreme hetero or homozygosity (ExcessHet > 20 and
165 InbreedingCoeff > 0.9) and high read strand bias (FS > 60 and SOR > 3). Then, we removed
166 calls for which up to 5% of genotypes had low quality (GQ < 20) and extreme coverage (GenDP
167 < 10 and GenDP > 40). We kept only bi-allelic sites, excluded SNPs on the heterozome (Super
168 scaffolds 13 and 42 [21]) and an exact Hardy-Weinberg test was used to remove sites that
169 significantly departed (p=0.05) from the expected equilibrium using the package
170 HardyWeinberg [27,28] in R [29], yielding a dataset of 6,448,521 SNP (mean individual coverage:
171 19.99X (sd: 4.38)). Lastly, we discarded singletons (minimum allelic count (mac) <2), yielding
172 to a total of 5,151,169 SNP for the population genomic analyses.
173
174 *SNP phasing and quality control*
175 The set of 6,448,521 variants was phased in two steps. First, individual variants were phased
176 using a read-based approach in which reads covering multiple heterozygous sites were used
177 to resolve local haplotypes. To do so, WhatsHap v1.0[30] was run independently for each
178 individual with default parameters. Secondly, variants were statistically phased with Shape-It
179 v4.1.2[31]. This algorithm integrates local individual phase and applies an approach based on
180 coalescence and recombination to statistically phase haplotypes and impute missing data.
181 Shape-It was run following the manual instructions for a better accuracy: the number of

conditioning neighbors in the PBWT was set to 8, and the MCMC chain was run with 10 burn-in generations, 5 pruning iterations, each separated by 1 burn-in iteration, and 10 main iterations.

To assess the quality of the phasing, we examined phase accuracy by using the switch-error-rate metric[32]. When comparing two phasing for an individual's variants, a switch error occurs when a heterozygous site has its phase switched relative to that of the previous heterozygous site. Thus, for each individual, we compared the *true* local phasing inferred form the read-based approach (WhatsHap) and the *statistical* phasing of this individual's variants statistically phased by Shape-It, with read-based phase information ignored only for the individual considered (same version and parameters than in the paragraph above). The final estimation of the switch error rate was done using the switchError code to compare both phasing sets (available at https://github.com/SPG-group/switchError) (fig. S1).

History of barn owls around the Mediterranean Sea

Population structure and genetic diversity

In order to investigate population structure among our samples, sNMF [33] was run for a number of clusters K ranging from 1 to 10 with 25 replicates for each K to infer individual clustering and admixture proportions. For this analysis, SNPs were pruned for linkage disequilibrium in PLINK v1.946 [34] (parameters --indep-pairwise 50 10 0.1) as recommended by the authors, yielding 594,355 SNP. Treemix [35] was used to calculate a drift-based tree of our populations, using this LD-pruned dataset. To detect admixture events between populations, 10 Treemix replicates were run for 0 to 10 migration events, with the tree rooted on the WC population, representative of a non-admixing population (see results, fig. S6).

Population expected and observed heterozygosity, population-specific private alleles, population-specific rare alleles (mac≤5) and population-specific total number of polymorphic sites were estimated using custom R scripts on the 5,151,169 variants dataset. To account for differences in sample sizes, which ranges from 4 to 10, population-specific statistics were calculated by randomly sampling 5 individuals from the larger populations (all except FR and SB) 10 times in a bootstrap-fashion and estimating the mean and standard deviation (SD). Individual-based relatedness (β) [36] and inbreeding coefficient for SNP data were calculated with the R package SNPRelate[37]. Overall F_{ST}, population pairwise F_{ST} and population specific F_{ST} [36] were computed with the hierfstat package v.0.5-9 [38]. Confidence intervals for population specific FST were computed by dividing the SNPs into 100 blocs, and bootstrapping 100 times 100 blocks with replacement. Finally, Principal Component Analyses (PCA) were also performed with the R package SNPRelate, first with all individuals and second only with the 66 European ones (excluding WC, CY and IS).

Haplotype sharing

To measure shared ancestry in the recent past between individuals, we ran fineSTRUCTURE [39] on the phased dataset including all individuals. For this analysis we initially modelled haplotype sharing between individuals using ChromoPainter to generate a co-ancestry matrix, which records the expected number of haplotypes chunks each individual donates to another. For this ChromoPainter step, we converted phased haps files to chromopainter phase files using the impute2chromopainter.pl script provided at http://www.paintmychromosomes.com and generated a uniform recombination map with the makeuniformrecfile.pl script. Using the version of ChromoPainter built into fineSTRUCTURE v.2.0.8, we performed 10 EM iterations to estimate the Ne and Mu

parameters (switch rate and mutation rate). The model was then run using the estimated values for these parameters (respectively 570.761 for Ne and 0.0074240 for Mu), and we used default settings to paint all individuals by all others (-a 0 0). We ran fineSTRUCTURE's MCMC model on the co-ancestry matrix for 500,000 burn-in and 500,000 sampling iterations, sampling every 10,000 iterations to determine the grouping of samples with the best posterior probability.

Modeling of history of European barn owl

Maximum-likelihood demographic inference

Data preparation

To describe the history of barn owls in Europe, we modeled five different demographic scenarios using fastsimcoal2 [40,41]. Given the position of Italy on the PCA (fig. 1e), its high F_{ST} and lower haplotype sharing with the rest of European populations (fig. 2), we tested in particular whether it could have been a cryptic glacial refugium during the last glaciation. To focus on European populations and due to computational constraints, we simplified the dataset to model the history of four populations of eight individuals (table S1): PT as representatives of the known refugium in the Iberian Peninsula [42]; IT and GR representing the peninsulas of Italy and Balkans, respectively; and CH, a product of the recolonization of northern Europe from the Iberian refugium[42].

Autosomal SNPs were filtered to retain only neutrally evolving regions by excluding SNPs found in genic regions and CpG mutations [43]. To achieve homogeneity among SNPs, we removed all sites with missing data and excluded positions with a coverage outside two thirds of the standard deviation of the mean. We employed a parsimony approach based on the Tytonidae phylogenetic tree [44] to determine the ancestral state of the SNPs using the

253 genomes of the two outgroups. Sites for which it was impossible to attribute a state based on
254 the available outgroups were discarded. The remaining 770,718 SNPs were used to produce
255 population pairwise site frequency spectra (SFS).
256
257 *Demographic scenarios and parameters*
258 Five different scenarios were tested to model the history of barn owls in continental Europe,
259 with a special focus on the period since the last glaciation (fig. 2, fig. S8). Three models
260 included only one refugium in the Iberian Peninsula and various possibilities of colonization
261 scenarios, thus excluding the persistence of barn owls in a second refugium during the
262 glaciation. The two last models included two refugia during the last glacial maximum (LGM),
263 a western refugium in the Iberian Peninsula and an eastern refugium, in the Italian Peninsula.
264 The models *1R-1*, *1R-2* and *1R-3* included only one refugium in the Iberian Peninsula. *1R-1*
265 model assumed only one colonization route around the north side of the Alps (forming the
266 CH population), and from there move southeast to reach first the Balkans (GR) and then Italy
267 (IT). The two other single-refugium models (*1R-2* and *1R-3*) assumed two distinct colonization
268 routes, one north of the Alps to CH and the other south of the Alps along the Mediterranean
269 coast to IT. *1R-2* assumes current Greece would have been colonized by owls from the Italian
270 Peninsula, following the route along the Mediterranean coast. In *1R-3*, Greece would have
271 been colonized via northern Europe, while the Mediterranean expansion would have stopped
272 in Italy.
273 The last two models included a second, eastern, refugium (*2R-1* and *2R-2*). In these models,
274 the western lineage expansion from the Iberian population would have colonized Europe
275 before the last glaciation, thus occupying all the Mediterranean peninsulas. During the last
276 glaciation, two distinct populations would have survived, respectively in the Iberian (western

277 refugium) and Italian (eastern refugium) Peninsulas. Both models assume that northern
278 Europe was recolonized from the Iberian lineage after the glaciation, but they differ in the
279 scenario of recolonization of southeastern Europe. In *2R-1*, Greece was recolonized from the
280 Italian refugium while in *2R-2* the expansion from the Iberian Peninsula would have
281 recolonized all eastern Europe, including current Greece. In this last scenario, the Italian
282 population would be the only relic from the eastern refugium. For all scenarios, migrations
283 between populations was allowed (see fig. 2 and table S2).
284 Wide search ranges for initial simulation parameters were allowed for population sizes,
285 divergence times and migration rates (table S2). Each population split was preceded by an
286 instantaneous bottleneck, in which the founding population size was drawn from a log-
287 uniform distribution between 0.01 and 0.5 proportion of current population sizes.
288
289 *Demographic inference*
290 Demographic simulations and parameter inference were performed under a composite-
291 likelihood approach based on the joint SFS as implemented in fastsimcoal2 [40,41]. For each of
292 the five scenarios, 100 independent estimations with different initial values were run. For
293 each run, there were 500000 coalescent simulations (option -n), with 50 expectation-
294 maximization (EM) cycles (-M and -L). As we do not have an accurate mutation rate for barn
295 owls, we fixed the end of the glaciation to 6000 generations BP (approximately 18'000 years
296 BP with a 3-year generation time) and scaled all other parameters relative to it using the -0
297 command option (using only polymorphic sites). The best-fitting scenario out of the five
298 tested was determined based on Akaike's information criterion [45] (AIC) and confirmed
299 through the examination of the likelihood ranges of each scenario as suggested in Kocher et
300 al. (1989)[46]. Non-parametric bootstrapping was performed to estimate 95% confidence

intervals (CI) of the inferred parameters under the best-fitting scenario. To account for LD, a block-bootstrap approach was employed as suggested by the authors [40,41]: the SNPs were divided into 100 same-size blocks, and then 100 bootstrap SFS were generated by sampling these blocks with replacement. Due to computational constraints, for bootstrapping we ran 50 independent parameter inferences per bootstrapped SFS with only 10 EM cycles each, instead of 50 cycles used for comparing scenarios above. This procedure has been defined as conservative [47], and is expected to produce quite large confidence intervals. We accepted this trade-off as our main goal was to determine the best demographic topology, accepting uncertainty on specific parameter values. The highest maximum-likelihood run for each bootstrapped SFS was used to estimate 95% CI of all parameters.

Niche modeling

In order to identify the regions of high habitat suitability for barn owls at the last glacial maximum (LGM, 20'000 years BP) and to support the demographic scenarios tested in the previous section, we modelled the past spatial distribution of the species in the Western Palearctic. We built species distribution model (SDM) using Maximum Entropy Modelling (MaxEnt), a presence-only based tool [48]. Current climatic variables for the Western Palearctic (fig. S10) were extracted from the WorldClim database at 5 arc min resolution using the R package rbioclim [49], and filtered to remove variables with a correlation of 0.8 or higher (fig. S9). The variables retained were: Mean Diurnal Range (Bio2), Min Temperature of Coldest Month (Bio6), Temperature Annual Range (Bio7), Mean Temperature of Wettest Quarter (Bio8), Precipitation Seasonality (Bio15), Precipitation of Driest Quarter (Bio17) and Precipitation of Coldest Quarter (Bio19). We built models with linear, quadratic and hinge features, and with a range (1 to 5) of regularization multipliers to determine which

combination optimized the model without over complexifying it. The best combination based on the corrected AIC (as recommended by Warren & Seifert [50]) was achieved with a quadratic model with 1 as regularization multiplier (table S5). We ran 100 independent maxent models, omitting 25% of the data during training to test the model. To avoid geographic bias due to different sampling effort in the distribution area of the species, we randomly extracted 1000 presence points within the IUCN distribution map [51] for each model run [52].

Predictive performances of the models were evaluated on the basis of the area under the curve (AUC) of the receiver operator plot of the test data. For all models with an AUC higher than 0.8 (considered a good model [53,54]), we transformed the output of Maxent into binary maps of suitability. We assigned a cell as suitable when its mean suitability value was higher than the mean value of the 10% test presence threshold. This conservative threshold allows us to omit all regions with habitat suitability lower than the suitability values of the lowest 10% of occurrence records. Finally, we averaged the values of the models for each cell, and only cells suitable in 90% of the models were represented as such in the map.

We projected the models to the climatic conditions of the mid-Holocene (6'000 years BP) and the LGM (20'000 years BP), which we extracted from WorldClim at the same resolution as current data. When projecting to past climates, the Multivariate Environmental Similarity Surface (MESS) approach [48] was used to assess whether models were projected into climatic conditions different from those found in the calibration data. As our goal was to highlight only areas of high suitability for barn owls, cells with climatic conditions outside the distribution used to build the model were assigned as unsuitable (0 attributed to cell with negative MESS). For each timepoint, the results of the models were merged and transformed into a binary map as described for current data (fig. 2c).

Barriers and corridors

Migration surface estimation in the western Palearctic

The Estimated Effective Migration Surface (EEMS) v.0.0.9 software [55] was used to visualize geographic regions with higher or lower than average levels of gene flow between barn owl populations of the Western Palearctic. Using the SNP dataset pruned for LD produced above, we calculated the matrix of genetic dissimilarities with the tool bed2diff. The free Google Maps api v.3 application available at http://www.birdtheme.org/useful/v3tool.html was used to draw the polygon outlining the study area in the Western Palearctic. EEMS was run with 1000 demes in five independent chains of 5 million MCMC iterations with a burn-in of 1 million iterations. Results were visually checked for MCMC chain convergence (fig. S11) and through the linear relation between the observed and fitted values for within- and between-demes estimates using the associated R package rEEMSplots v.0.0.1 [55]. With the same package, we produced a map of effective migration surface by merging the five MCMC chains.

Isolation by distance in continental Europe

To investigate how population structure correlated with spatial distances between European populations and to detail the role of the Alps as a barrier to gene flow, we performed Mantel tests as implemented in the ade4 package v.1.7-15 [56] for R. We compared the genetic distances (pairwise F_{ST} between populations, see section *Population Structure and Genetic Diversity* for details) with different measures of geographical distance between populations: the shortest distance over land via direct flight and the distance constrained by the presence of the Alps, forcing the connection of the Italian population to the other populations via the Greek Peninsula (fig. S13). We also tested the linear regression between both variables in R.

Results

History of barn owls around the Mediterranean Sea

Genetic diversity and population structure in the Western Palearctic

Despite an overall low differentiation (overall F_{ST}=0.047, comparable with the overall FST=0.045 estimated by Burri et al. [20]), the dataset revealed a structuration of the genetic diversity among barn owls of the Western Palearctic. The first axis of the genomic PCA (explaining 3.32% of the total variance) contrasted individuals from the Levant populations (IS and CY) to all other individuals (fig. 1d), consistent with K=2 being the best estimate in sNMF (fig. S4, fig. S5). For K=3 (fig. 1b), the Canary population (WC) formed an independent genetic cluster, and this was confirmed by the second axis of the PCA (explaining 2.6% of the variance) opposing it to all other individuals (fig. 1d, fig. S2). This isolation of WC was also observable in table 1, with a lot of privates and rare alleles in Tenerife island, it's higher F_{IT} and the highest population specific F_{ST} of all sampled populations. On the same PCA (fig. 1d), individuals from European populations (FR, CH, DK, IT, SB, GR, AE) formed a third distinct cluster, matching their grouping in a single cluster at K=3 with sNMF (fig. 1b). The Iberian individuals (PT) occupied a central position on the PCA (around 0 on both axes) and a mixed composition in sNMF (fig. 1b). This central position of the Iberian population was also visible in the pairwise F_{ST}, where the highest value in the pairs involving PT is 0.055 (with both CY and WC) while all other pairwise comparisons involving populations from two of the distinct groups identified before (Levant, Canary Islands and Europe) have values equal or higher (fig. 1c). The TreeMix analysis (fig. 1f) was also consistent with these results, since it also identified these major lineages, first isolating the Canary population in a specific lineage, then grouping

395 the Levant populations (IS and CY) in a second lineage and finally all European populations in
396 a third lineage. In Europe, the Iberian population was basal to all other populations.
397
398 *Population structure in continental Europe*
399 Focusing only on European samples, southern populations (PT, IT, GR and AE) harbored a
400 higher genetic diversity than northern populations (CH, FR, DK, SB) (table 1). The first axis of
401 the genomic PCA based on samples from European-only populations opposed the Italian
402 individuals to all others (fig.1e, fig. S3). This isolation of Italian samples was also apparent in
403 the pairwise F_{ST} within Europe, with all the largest values involving IT. These results were
404 consistent with sNMF on all samples for K higher than 3, where IT individuals formed an
405 independent genetic cluster (fig. S5, illustrated in fig. 1a), as well as TreeMix, where the Italian
406 population was the first to split and had the longest branch within European lineage (fig. 1f).
407 Consistently with the distribution of the individuals in the European PCA (fig. 1e, fig. S3), the
408 ancestry coefficients in the sNMF analyze of k=4 and k=5 (fig. S5) revealed the genetic
409 differentiation of northern populations (FR, CH and DK) compared to the Italian one, also
410 opposed in the first axis. Individuals from GR and AE individuals shared ancestry with both
411 western and Italian population, in line with their central position along this first axis of the
412 European PCA. For k=5, a third European component was distinguished in the Aegean
413 individuals. This component was the majoritarian in Greek samples with contributions of both
414 northern and Italian component; and Serbian samples appeared as a mix of the northern and
415 the Aegean component. The eastern lineage (CY and IS), grouped at previous K, were split
416 into two distinct ancestry pools at K=6 (fig. 1a). AE individuals harbored low amounts of CY
417 ancestry, absent in all other European populations, and two CY individuals carried a large
418 contribution of the Aegean component. Consistently, the first migration event detected by

419 TreeMix was from CY, a population from the Levant lineage, to AE, a population from the
420 European lineage (fig. 1f).
421
422 *Fine Structure and Haplotype sharing*
423 The clustering of individuals by FineStructure, based on shared haplotypes between
424 individuals was consistent with previous results (fig. S7). Individuals from the different
425 populations sampled were monophyletic, except for CH and FR individuals, mixed in the same
426 population. Consistently with this grouping, haplotypes from any given population were more
427 likely to be found in individuals from the same population, followed by its most related
428 populations (fig. 2). In the Levant lineage, IS haplotypes mostly painted IS Individuals but also
429 CY individuals and vice versa. Iberian haplotypes mostly painted PT individuals, but also
430 contributed greatly to the painting of all European individuals, decreasing with distance.
431 Western European haplotypes (from FR and CH) mostly painted western European
432 individuals, then northern individuals (from DK) and finally eastern individuals (from SB, GR
433 and AE). The reverse pattern was observed for haplotypes from eastern Europe (GR, AE), with
434 a gradient of contribution decreasing from east to west. Haplotypes from DK and SB mostly
435 painted individuals from their own population, but also in their respective neighbors in both
436 eastern and western European populations. Italian haplotypes were the most distinct
437 haplotypes among European populations, mostly painting Italian individuals, followed by
438 Greek individuals, and being painted by other populations at a lower rate than expected given
439 its geographic position. Finally, AE haplotypes also painted more often CY individuals than IS
440 individuals. This painting of levant individuals by AE haplotypes was higher than the
441 contribution from any other European individual, and both CY and IS haplotypes painted more
442 AE individuals than any other European individual.

Modeling of the history of European barn owls

Species distribution modeling

Habitat suitability projections showed that, from a climatic point of view, there were suitable regions for barn owls all around the Mediterranean Sea during the glaciation (20'000 years BP; fig. 3c). Large areas were suitable in northern Africa and the Iberian Peninsula, but also in the two eastern Mediterranean peninsulas (current Italy and Greece). At this point, the sea levels were lower than today's and the two eastern peninsulas were more connected, allowing for a continuous region of suitable barn owl habitat. At the mid-Holocene (6'000 years BP), major changes in sea level revealed a coastline very similar to nowadays. Our projections revealed a reduction of habitat suitability in northern Africa at this time, while the suitability of western and northern Europe increased (fig. 3c). Finally, today, nearly all continental Europe is suitable for the barn owls, with the notable exception of mountain areas (fig. 3c).

Demographic inference

AIC and raw likelihood comparisons showed that the two refugia model *2R-1* explains best the SFS of our dataset (table S3; Fig. 3b). In this model, an ancestral Italian lineage (IT) split from the Iberian lineage (PT) before the last glaciation, estimated at approximately 69'000 years BP (95% CI: 24'000-90'000 years BP; calculated with 3-year generation time). After its initial expansion, the ancestral population is estimated to have been larger in the Italian Peninsula that in Iberia (respectively 189K (11K-320k) and 11k (10K-73k) haploid individuals). During the glaciation (fixed between 24 and 18K years BP), both populations experienced a bottleneck, with a population size reduced to 6.8k (1.2k-141k) individuals in the Iberian

lineage and 62 (36-116k) in the Italian. After the glaciation, the size of both populations increased to their current size, estimated at 44k (20K-380k) in the Iberian Peninsula and 1.3k (1k-326k) in the Italian Peninsula, both smaller but consistent with their estimated census size (55k-98k [57,58] and 6k-13k [59], respectively). The Greek population split from the Italian branch around 5'700 years BP while the Swiss (CH) population split slightly later from Iberia (5'000 years BP) and maintain a high level of gene flow (estimated to 90 (46-1.4k) from CH to PT and 8 (3-62) in the reverse direction). Current effective population sizes of the CH and GR populations are estimated to 3.4k (1k-205k) and 1.4k (1k-208k), respectively (fig. 2b), in line with census results (1000-2500 [60] and 3000-6000 [61], respectively). Migration between these populations is estimated to be highest from IT and GR to CH (respectively 27 (0.2-157) migrants from IT and 42 (0.1-156) from GR) and lowest in the opposite direction (respectively 1.3 (0.1-96) migrants from CH to GR and 0.02 (0.2-38) from CH to IT) (table S4). Point estimates with 95% confidence intervals for all parameters of the best model are given in (table S4), as well as single point estimates for all models (table S2).

Barriers and corridors

Migration Surface Estimate in the Western Palearctic

Estimated Effective Migration Surface identified large water bodies, especially in the eastern Mediterranean and around Cyprus, as regions resisting to migration (fig. S12). On the mainland, barriers to gene flow matched the main formations of the Alpide belt in the region, an orogenic formation spanning from western Europe to eastern Asia. From west to east, a light barrier overlapped with the Pyrenees, a strong barrier spanned the Alps to the Balkans and a third obstacle matched the Taurus mountains in Anatolia. A region with high gene flow

was identified in continental Europe above the Alps, spanning from western Europe to the Balkan Peninsula.

Isolation by distance in Europe

In continental Europe, the shortest path overland did not correlate significantly with genetic distance (fig. S13) (mantel test, p-value = 0.193, R = 0.20 / linear model, p-value = 0.26, R^2 = 0.012). On the contrary, when the geographic distance between populations included the barrier formed by the Alps (i.e. the Italian population was connected to other populations via the Greek Peninsula, itself connected to western Europe via northern Europe), both tests were significant (mantel test, p-value = 0.002, R = 0.68 / linear model, p-value = 1.3×10^{-5}, R^2 = 0.507).

501 Discussion

502

503 The history of natural populations is shaped by the combination of landscape barriers and
504 climatic variations that isolate and mix lineages through their combined actions. Consistently
505 with previous work [20], we show that barn owls colonized the Western Palearctic in a ring-like
506 fashion around the Mediterranean Sea, with one arm around the Levant and the second
507 throughout Europe. However, using whole genome sequences we found this colonization
508 actually predates the last glaciation and pinpoint a narrow secondary contact zone between
509 the two lineages in Anatolia rather than in the Balkans. In addition, we provide evidence that
510 barn owls recolonized Europe after the LGM from two distinct glacial refugia – a western one
511 in Iberia and an eastern in Italy – rather than a single one as it was previously thought. As
512 temperatures started rising, western and northern Europe were colonized by owls from the
513 Iberian Peninsula while, in the meantime, the eastern refugium population of Italy had spread
514 to the Balkans (fig. 4). The western and eastern glacial populations finally met in eastern
515 Europe. This complex history of populations questions the taxonomy of the multiple *Tyto alba*
516 subspecies, highlights the key roles of mountain ranges and large water bodies as barriers to
517 gene flow for a widespread bird and illustrates the power of population genomics in
518 unraveling intricate patterns.

519

520 *Colonization of the Western Palearctic and gene flow in Anatolia*

521 Our results show that two distinct barn owl genetic lineages surround the Mediterranean
522 Basin: one in the Levant, and a second in Europe (fig. 1b, 1c, 1d, 1f), likely connected via
523 northern Africa. Supported by the higher and specific diversity of the basal population of each
524 arm (namely, IS and PT; table 1), these observations are consistent with the ring colonization

525 scenario hypothesized by Burri et al. [20]. However, we show that a barn owl population
526 survived the last glaciation in Italy (see next section for details) and that its genetic makeup
527 resembles the European lineage (fig. 1b, 1d, 1f). Therefore, the ring colonization of Europe
528 around the Mediterranean appears to have been pre-glacial, whereas the post-glacial history
529 is more convoluted (see next section).
530 In previous studies, the ancestry of Greek and Aegean populations was unclear, with a
531 hypothesized mixed origin between the European and Levant lineages [20]. This uncertainty was
532 mostly likely due to the low resolution of genetic markers (Mitochondrial DNA and
533 microsatellites), as the genomic data reported here clearly show that Greek and Aegean owls
534 are genetically much closer to European than to Levant ones (fig. 1b, 1c, 1d, 1f). This
535 observation indicates that the European lineage reached further east than previously
536 assumed, allowing us to pinpoint the secondary contact zone between the European and
537 Levant lineages to Anatolia, instead of the Balkans as it had been proposed. In Anatolia, the
538 Taurus and Zagros mountain ranges form an imposing barrier that appears to have stopped
539 the expansion of the Levant lineage both during the ring colonization and nowadays.
540 Despite the barrier, and although we do not see a complete admixture of the two lineages,
541 there is evidence of some gene flow. Indeed, the first migration in Treemix (fig. 1f) pointed to
542 a secondary contact between CY and AE, consistent with the signals of admixture between
543 these populations (fig. 1a, 1b, 2). The admixture pattern however is restricted geographically
544 to this narrow region and does not permeate further into either of the lineages, as
545 surrounding populations (IS in the Levant and GR and SB in Europe) do not show signals of
546 admixture (fig. 1, 2). Thus, the migration between populations on both sides seems limited
547 and possibly only occurs along a narrow corridor along the Turkish coast where only a few

548 barn owls have been recorded [62]. Further analyses with samples from Anatolia should allow
549 to characterize in high resolution how and when admixture occurred in this region.
550
551 *Glacial refugia and recolonization of Europe*
552 Previous studies showed that barn owls survived the last glaciation by taking refuge in the
553 Iberian Peninsula and maybe even in emerged land in the Bay of Biscay [21,42]. The observed
554 distribution of diversity in Europe, and especially the specific makeup of the Italian
555 populations, is best explained by a demographic model with two glacial refugia – one in Iberia
556 and a second in Italy, derived from the Iberian population before the glaciation (fig. 3a and
557 3b; table S5). Environmental projections not only support this model, as Italy was highly
558 suitable for the species at the time, but also show that, due to the low levels of the Adriatic
559 Sea, the suitable surface extended to the west coast of the Balkans (LGM - fig. 3c). Crucially,
560 three of the barn owl's key prey also had glacial refugia in the Italian and Balkan peninsulas,
561 namely the common vole (*Microtus* sp.) [63], the wood mouse (*Apodemus* sp.) [64] and shrews
562 (*Crocidura* sp.) [65]. The inferred size of the pre-glacial population of barn owls inhabiting
563 current Italy was larger than any other (189k (11K-320K)), prior to a strong bottleneck during
564 the glaciation (population reduced to 62 individuals (36-116k)). These values are likely
565 inflated by necessary simplification of the model (e.g. instant bottlenecks) or by gene flow
566 from unmodeled/unsampled populations, for example from the Levant lineage to eastern
567 European populations (GR), or from northern Africa to Italy via Sicily. The latter would have
568 been facilitated by the increased connectivity between Italy and North Africa during the
569 glaciation (fig. 3c) [66,67,68].
570 With the warming following the LGM, Europe became gradually more suitable and, by the
571 mid-Holocene (6000 years ago), most of western and northern Europe were appropriate for

572 barn owls (fig. 2b) as well as the common vole (*Microtus arvalis*) [69]. The genetic similarity
573 between Iberian (PT) and northwestern populations (CH, FR, DK; fig. 1a, 1e) indicates that
574 barn owls colonized these newly available regions from the Iberian refugium as previously
575 thought [42]. The contribution from the Italian refugium to northern populations appears to
576 have been hindered by the Alps (see next sections), as suggested by the higher genetic
577 distance between them (fig. 1a, 1c, 1d and 2). Instead, at this time the Adriatic Sea had neared
578 today's levels, isolating genetically and geographically the Italian refugium from its
579 component in the Balkan Peninsula (fig. 3b – IT-GR split ~6k fig. 3b and fig. 3c). Only more
580 recently did the rise of temperatures allow for areas in the east of Europe to become suitable,
581 finally connecting the southeastern populations near the Aegean Sea (GR and AE) with
582 populations in the northeastern part of Europe (fig. 3c). In particular, the high heterozygosity
583 and admixed ancestry of Serbian individuals (table 1, fig. 1a) suggest that the suture between
584 the Iberian and the Italo-Greek glacial lineages took place in eastern Europe. This newly
585 identified postglacial recolonization scheme of continental Europe by the barn owl matches
586 the general pattern described for the brown bear (*Ursus arctos*) and shrew (*Sorex* sp.) [7].
587 The isolation by distance pattern observed between European populations (fig. S13)
588 highlights a diffusion of alleles in the European populations rather than a narrow hybrid zone.
589 Further, the inferred migration rates support high current gene flow in the region (fig. 3b, CH
590 and GR in table S4), and we found signals of each ancestry in populations far from the suture
591 zone (dark blue in GR and light blue in CH and DK, fig. 1a). Finally, the measure of haplotype
592 sharing decreases consistently with distance between populations around the northern side
593 of the Alps between populations from Iberia to Greece, excluding IT (fig. 2). Surrounded by
594 the sea and the Alps, Italy is the exception and appears to have avoided incoming gene flow
595 (fig. S12, isolation in fig. 2), thus being a better-preserved relic of the refugium population

596 (own cluster in sNMF K>4, fig. S5). In contrast, the Balkan component admixes smoothly with
597 the other European populations. Such seamless mixing of the two glacial lineages from
598 southern refugia where barn owls are mostly white [20,70], brings further into question the
599 subspecies *T. a. guttata*.
600
601 *The case of Tyto alba guttata*
602 Traditionally, in Europe, the eastern barn owl (*T. a. guttata* (Brehm, CL, 1831)) is defined by
603 its dark rufous ventral plumage in contrast to the white western barn owl (*T. a. alba* (Scopoli,
604 1769)) [71]. With a wide distribution, it is recorded from The Netherlands to Greece, including
605 most of northern and eastern Europe [72]. However, this repartition does not match the history
606 of any specific glacial lineage identified above, nor any genetically differentiated population.
607 The dark populations of northern Europe (DK) are genetically as similar to lighter western
608 populations (FR, CH) than to the dark ones in the east (SB). This color variance within
609 European populations has been shown to be maintained through local adaptation [70], and
610 while the genomic basis and history of this trait remain worthy of future investigations, we
611 suggest that all European barn owls form a single subspecies (*T. a. alba)*, reflecting the entire
612 European population, regardless of their color.
613
614 *Barriers and corridors shape the connectivity of the Western Palearctic meta-population*
615 The partition of genetic diversity among barn owls in the Western Palearctic allowed us to
616 identify barriers and corridors to gene flow. Populations isolated by large water bodies have
617 accumulated substantial genetic differences as, for example, the higher F_{ST} in the Canary and
618 Cyprus islands (fig. 1c, table 1), and reflect the importance of water as a barrier to dispersion
619 in this species [21]. On the mainland, and as described for the American barn owl [73], major

620 mountain ranges act as significant obstacles to migration for European barn owls and can
621 generate genetic structure. First, the high mountain ranges of Taurus and Zagros coincide
622 with the contact zone between the Levant and the European lineages both nowadays and
623 potentially at the time of the pre-glacial ring colonization of Europe (see above). Second, the
624 Alps and the Balkan Mountains slowed the northward expansion of the glacial populations of
625 Italy and Greece after the LGM and still constrain migration between populations on both
626 sides of their ranges. If these results remain to be confirmed with observational data (i.e.
627 ringing data not available for all countries), they emphasize that, despite its worldwide
628 repartition and its presence on many islands, the connectivity of barn owl populations is
629 heavily driven by biogeographical barriers.
630
631 Conclusion
632
633 The combination of whole genome sequencing and sophisticated modeling methods revealed
634 the complex history of the barn owl in the Western Palearctic with a precision previously
635 unachievable. It allowed the localization of a secondary contact zone as well as the discovery
636 of a cryptic glacial refugium. However, several questions remain unanswered, awaiting for
637 relevant samples to be collected and analyzed: What role did northern African populations
638 played in connecting the Levant and European lineages? Did they contribute to the diversity
639 observed in Italy? How narrow is the contact zone between the Levant and European lineages
640 in Anatolia? Lastly, the origin of barn owls from the Western Palearctic as a whole also
641 deserves further investigation, as they are believed to have colonized the Western Palearctic
642 from the east, given the species' supposed origin in southeastern Asia approximately 4 million
643 years ago. But this is at odds with the higher genetic diversity of the Iberian population

644 compared to the Levant one. Such inconsistency points to the need for samples from around
645 the world, to understand how this charismatic group of nocturnal predators conquered the
646 entire planet.
647 Research on postglacial recolonization and the subsequent phylogeographic patterns peaked
648 at the turn of the century, with many studies providing an overview of the history of a wide
649 variety of organisms (reviewed by Hewitt[7]). The rise in availability of genomic data for non-
650 model species, combined with the type of approaches used here, will rewrite the history of
651 many of them. Furthermore, it will allow to detail the genomic consequences of such history
652 both from a neutral and selective perspective. Applied to several species, these approaches
653 will redefine with greater clarity the broad phylogeographical patterns in the Western
654 Palearctic and elsewhere, to re-think taxonomic classifications and to better understand how
655 organisms might adapt to a changing environment in a complex, fragmented and rapidly
656 changing landscape.

657 Acknowledgements

658

659 We thank the following institutions and individuals for providing samples or aiding in
660 sampling: The European Barn Owl Network, Sylvain Antoniazza and Reto Burri, the Natural
661 History Museum of Tenerife, the Wildlife Rehabilitation Centre La Tahonilla (Cabildo Insular
662 de Tenerife), Kristijan Ovari and the Palić Zoo (Serbia). We thank Céline Simon and Luis San-
663 José for their valuable assistance with molecular work as well as Alexandros Topaloudis for
664 scripts. Finally, we also thank Olivier Delaneau for his advice on the phasing of the individuals
665 and its evaluation. This study was funded by the Swiss National Science Foundation with
666 grants 31003A-138180 & 31003A_179358 to JG and 31003A_173178 to AR.

667

668 Data Accessibility

669 The raw Illumina reads for the whole-genome sequenced individuals are available in
670 BioProject PRJNA700797 and BioProject PRJNA727977.

671

672 Author Contribution

673

674 TC, APM, AR, JG designed this study; GD and APM produced whole-genome resequencing
675 libraries and called the variants; TC and APM conducted the analyses; KD, RL, JL, HDM, PB,
676 VB, MC, KD, HDM, NK, RL, FM, KO, LP, MR and FS provided samples to the study; TC led the
677 writing of the manuscript with input from APM and all authors.

678 References

679 1. Huntley, B. & Webb, T. Migration: Species' Response to Climatic Variations Caused by
680 Changes in the Earth's Orbit. *J. Biogeogr.* **16**, 5–19 (1989).
681 2. Irwin, D. E., Irwin, J. H. & Price, T. D. Ring species as bridges between microevolution and
682 speciation. *Genetica* **112**, 223–243 (2001).
683 3. Devitt, T. J., Baird, S. J. & Moritz, C. Asymmetric reproductive isolation between terminal
684 forms of the salamander ring species Ensatina eschscholtzii revealed by fine-scale genetic
685 analysis of a hybrid zone. *BMC Evol. Biol.* **11**, 245 (2011).
686 4. Pereira, R. J., Monahan, W. B. & Wake, D. B. Predictors for reproductive isolation in a ring
687 species complex following genetic and ecological divergence. *BMC Evol. Biol.* **11**, 194
688 (2011).
689 5. Cacho, N. I. & Baum, D. A. The Caribbean slipper spurge Euphorbia tithymaloides: the first
690 example of a ring species in plants. *Proc. R. Soc. B Biol. Sci.* **279**, 3377–3383 (2012).
691 6. Stöck, M. *et al.* Cryptic diversity among Western Palearctic tree frogs: Postglacial range
692 expansion, range limits, and secondary contacts of three European tree frog lineages
693 (Hyla arborea group). *Mol. Phylogenet. Evol.* **65**, 1–9 (2012).
694 7. Hewitt, G. M. Post-glacial re-colonization of European biota. *Biol. J. Linn. Soc.* **68**, 87–112
695 (1999).
696 8. Hewitt, G. The genetic legacy of the Quaternary ice ages. *Nature* **405**, 907–913 (2000).
697 9. Willeit, M., Ganopolski, A., Calov, R. & Brovkin, V. Mid-Pleistocene transition in glacial
698 cycles explained by declining CO2 and regolith removal. *Sci. Adv.* **5**, eaav7337 (2019).
699 10. Clark, P. U. *et al.* The Last Glacial Maximum. *Science* **325**, 710–714 (2009).
700 11. Can secondary contact following range expansion be distinguished from barriers to gene
701 flow? [PeerJ]. https://peerj.com/articles/5325/.
702 12. Boucher, F. C., Zimmermann, N. E. & Conti, E. Allopatric speciation with little niche
703 divergence is common among alpine Primulaceae. *J. Biogeogr.* 12 (2015).
704 13. Tomasello, S., Karbstein, K., Hodač, L., Paetzold, C. & Hörandl, E. Phylogenomics unravels
705 Quaternary vicariance and allopatric speciation patterns in temperate-montane plant
706 species: A case study on the Ranunculus auricomus species complex. *Mol. Ecol.* **29**, 2031–
707 2049 (2020).
708 14. Capblancq, T., Després, L., Rioux, D. & Mavárez, J. Hybridization promotes speciation in
709 Coenonympha butterflies. *Mol. Ecol.* **24**, 6209–6222 (2015).
710 15. Hey, J. The Divergence of Chimpanzee Species and Subspecies as Revealed in
711 Multipopulation Isolation-with-Migration Analyses. *Mol. Biol. Evol.* **27**, 921–933 (2010).
712 16. Linck, E., Freeman, B. G. & Dumbacher, J. P. Speciation and gene flow across an elevational
713 gradient in New Guinea kingfishers. *J. Evol. Biol.* **33**, 1643–1652 (2020).
714 17. Poelstra, J. W. *et al.* The genomic landscape underlying phenotypic integrity in the face of
715 gene flow in crows. *Science* **344**, 1410–1414 (2014).
716 18. Rougemont, Q. *et al.* Demographic history shaped geographical patterns of deleterious
717 mutation load in a broadly distributed Pacific Salmon. *PLOS Genet.* **16**, e1008348 (2020).

19. Duranton, M. *et al.* The origin and remolding of genomic islands of differentiation in the European sea bass. *Nat. Commun.* **9**, 2518 (2018).
20. Burri, R. *et al.* The genetic basis of color-related local adaptation in a ring-like colonization around the Mediterranean: GENETICS OF CIRCUM-MEDITERRANEAN COLOR ADAPTATION. *Evolution* **70**, 140–153 (2016).
21. Unexpected post-glacial colonisation route explains the white colour of barn owls (Tyto alba) from the British Isles | bioRxiv. https://www.biorxiv.org/content/10.1101/2021.04.23.441058v1.
22. Van der Auwera, G. A. *et al.* From FastQ data to high confidence variant calls: the Genome Analysis Toolkit best practices pipeline. *Curr. Protoc. Bioinforma.* **43**, 11.10.1-11.10.33 (2013).
23. Trimmomatic: a flexible trimmer for Illumina sequence data | Bioinformatics | Oxford Academic. https://academic.oup.com/bioinformatics/article/30/15/2114/2390096.
24. Li, H. & Durbin, R. Fast and accurate short read alignment with Burrows-Wheeler transform. *Bioinforma. Oxf. Engl.* **25**, 1754–1760 (2009).
25. ANGSD: Analysis of Next Generation Sequencing Data | BMC Bioinformatics | Full Text. https://bmcbioinformatics.biomedcentral.com/articles/10.1186/s12859-014-0356-4.
26. Danecek, P. *et al.* The variant call format and VCFtools. *Bioinforma. Oxf. Engl.* **27**, 2156–2158 (2011).
27. Graffelman, J. & Camarena, J. M. Graphical tests for Hardy-Weinberg equilibrium based on the ternary plot. *Hum. Hered.* **65**, 77–84 (2008).
28. Graffelman, J. Exploring Diallelic Genetic Markers: The HardyWeinberg Package. *J. Stat. Softw.* **64**, 1–23 (2015).
29. Team, R. C. *R: A language and environment for statistical computing (3.5. 1)[Computer software]. R Foundation for Statistical Computing*. (2020).
30. Martin, M. *et al.* WhatsHap: fast and accurate read-based phasing. *bioRxiv* 085050 (2016) doi:10.1101/085050.
31. Delaneau, O., Zagury, J.-F., Robinson, M. R., Marchini, J. L. & Dermitzakis, E. T. Accurate, scalable and integrative haplotype estimation. *Nat. Commun.* **10**, 5436 (2019).
32. Choi, Y., Chan, A. P., Kirkness, E., Telenti, A. & Schork, N. J. Comparison of phasing strategies for whole human genomes. *PLOS Genet.* **14**, e1007308 (2018).
33. Fast and Efficient Estimation of Individual Ancestry Coefficients. https://www.ncbi.nlm.nih.gov/pmc/articles/PMC3982712/.
34. PLINK: A Tool Set for Whole-Genome Association and Population-Based Linkage Analyses. https://www.ncbi.nlm.nih.gov/pmc/articles/PMC1950838/.
35. Pickrell, J. K. & Pritchard, J. K. Inference of Population Splits and Mixtures from Genome-Wide Allele Frequency Data. *PLoS Genet.* **8**, e1002967 (2012).
36. Weir, B. S. & Goudet, J. A Unified Characterization of Population Structure and Relatedness. *Genetics* **206**, 2085–2103 (2017).
37. Zheng, X. *et al.* A high-performance computing toolset for relatedness and principal component analysis of SNP data. *Bioinformatics* **28**, 3326–3328 (2012).

759 38. Goudet, J. hierfstat, a package for r to compute and test hierarchical F-statistics. *Mol. Ecol.*
760 *Notes* **5**, 184–186 (2005).
761 39. Lawson, D. J., Hellenthal, G., Myers, S. & Falush, D. Inference of Population Structure using
762 Dense Haplotype Data. *PLoS Genet.* **8**, e1002453 (2012).
763 40. Excoffier, L. & Foll, M. fastsimcoal: a continuous-time coalescent simulator of genomic
764 diversity under arbitrarily complex evolutionary scenarios. *Bioinformatics* **27**, 1332–1334
765 (2011).
766 41. Excoffier, L., Dupanloup, I., Huerta-Sánchez, E., Sousa, V. C. & Foll, M. Robust
767 Demographic Inference from Genomic and SNP Data. *PLOS Genet.* **9**, e1003905 (2013).
768 42. Antoniazza, S. *et al.* Natural selection in a postglacial range expansion: the case of the
769 colour cline in the European barn owl. *Mol. Ecol.* **23**, 5508–5523 (2014).
770 43. Background selection and biased gene conversion affect more than 95% of the human
771 genome and bias demographic inferences | eLife.
772 https://elifesciences.org/articles/36317.
773 44. Uva, V., Päckert, M., Cibois, A., Fumagalli, L. & Roulin, A. Comprehensive molecular
774 phylogeny of barn owls and relatives (Family: Tytonidae), and their six major Pleistocene
775 radiations. *Mol. Phylogenet. Evol.* **125**, 127–137 (2018).
776 45. Akaike, H. A New Look at the Statistical Model Identification. in *Selected Papers of*
777 *Hirotugu Akaike* (eds. Parzen, E., Tanabe, K. & Kitagawa, G.) 215–222 (Springer, 1998).
778 doi:10.1007/978-1-4612-1694-0_16.
779 46. Kocher, T. D. *et al.* Dynamics of mitochondrial DNA evolution in animals: amplification and
780 sequencing with conserved primers. *Proc. Natl. Acad. Sci.* **86**, 6196–6200 (1989).
781 47. Malaspinas, A.-S. *et al.* A genomic history of Aboriginal Australia. *Nature* **538**, 207–214
782 (2016).
783 48. Elith, J. *et al.* A statistical explanation of MaxEnt for ecologists. *Divers. Distrib.* **17**, 43–57
784 (2011).
785 49. M. Exposito-Alonso. rbioclim: Improved getData function from the raster R package to
786 interact with past, present and future climate data from worldclim.org. (2017).
787 50. Warren, D. L. & Seifert, S. N. Ecological niche modeling in Maxent: the importance of
788 model complexity and the performance of model selection criteria. *Ecol. Appl.* **21**, 335–
789 342 (2011).
790 51. BirdLife International. The IUCN Red List of Threatened Species. Version 6.2. (2019).
791 52. Fourcade, Y. Comparing species distributions modelled from occurrence data and from
792 expert-based range maps. Implication for predicting range shifts with climate change.
793 *Ecol. Inform.* **36**, 8–14 (2016).
794 53. Swets, J. A. Measuring the accuracy of diagnostic systems. *Science* **240**, 1285–1293 (1988).
795 54. Li, Y., Li, M., Li, C. & Liu, Z. Optimized Maxent Model Predictions of Climate Change
796 Impacts on the Suitable Distribution of Cunninghamia lanceolata in China. *Forests* **11**, 302
797 (2020).
798 55. Petkova, D., Novembre, J. & Stephens, M. Visualizing spatial population structure with
799 estimated effective migration surfaces. *Nat. Genet.* **48**, 94–100 (2016).

56. Dray, S. & Dufour, A.-B. The ade4 Package: Implementing the Duality Diagram for Ecologists. *J. Stat. Softw.* **22**, 1–20 (2007).
57. Lourenço, R., Roque, I., Tomé, R. & Sepúlveda, P. Current status and distribution of nocturnal birds (Strigi- formes and Caprimulgiformes) in Portugal. 16.
58. Martí R and del Moral C (eds). *Atlas de las aves reproductoras de España.* (2003).
59. Ornitologia Italiana - Vol.3 - Stercorariidae Caprimulgidae - Brichetti Pierandrea; Fracasso Giancarlo | Libro Alberto Perdisa Editore 06/2005 - HOEPLI.it. *www.hoepli.it* https://www.hoepli.it/libro/ornitologia-italiana-vol3-stercorariidae-caprimulgidae/9788883722417.html.
60. 9783952106457: Atlas des oiseaux nicheurs de Suisse : Distribution des oiseaux nicheurs en Suisse et au Liechtenstein en 1993-1996 - AbeBooks - Hans Schmid; Roland Luder; Beat Naef-Daenzer; Roman Graf; Niklaus Zbinden: 3952106453. https://www.abebooks.fr/9783952106457/Atlas-oiseaux-nicheurs-Suisse-Distribution-3952106453/plp.
61. Birds in Europe: Population Estimates, Trends and Conservation Status | BirdLife. https://www.birdlife.org/europe-and-central-asia/news/birds-europe-population-estimates-trends-and-conservation-status.
62. Göçer, E. & Johnson, D. H. The Barn owl (Tyto alba) in Turkey. **7(3-4): 500-506**, (2018).
63. Stojak, J., Borowik, T., Górny, M., McDevitt, A. D. & Wójcik, J. M. Climatic influences on the genetic structure and distribution of the common vole and field vole in Europe. *Mammal Res.* **64**, 19–29 (2019).
64. Herman, J. S. *et al.* Post-glacial colonization of Europe by the wood mouse, Apodemus sylvaticus: evidence of a northern refugium and dispersal with humans. *Biol. J. Linn. Soc.* **n/a**,.
65. Dubey, S. *et al.* Molecular evidence of Pleistocene bidirectional faunal exchange between Europe and the Near East: the case of the bicoloured shrew (Crocidura leucodon, Soricidae). *J. Evol. Biol.* **20**, 1799–1808 (2007).
66. Dapporto, L. & Bruschini, C. Invading a refugium: post glacial replacement of the ancestral lineage of a Nymphalid butterfly in the West Mediterranean. *Org. Divers. Evol.* **12**, 39–49 (2012).
67. Husemann, M., Schmitt, T., Zachos, F. E., Ulrich, W. & Habel, J. C. Palaearctic biogeography revisited: evidence for the existence of a North African refugium for Western Palaearctic biota. *J. Biogeogr.* **41**, 81–94 (2014).
68. Lodolo, E. *et al.* Post-LGM coastline evolution of the NW Sicilian Channel: Comparing high-resolution geophysical data with Glacial Isostatic Adjustment modeling. *PLOS ONE* **15**, e0228087 (2020).
69. Heckel, G., Burri, R., Fink, S., Desmet, J.-F. & Excoffier, L. Genetic Structure and Colonization Processes in European Populations of the Common Vole, Microtus Arvalis. *Evolution* **59**, 2231–2242 (2005).

70. Antoniazza, S., Burri, R., Fumagalli, L., Goudet, J. & Roulin, A. Local adaptation maintains Clinal variation in melanin-based coloration of Euopean barn owl (Tyto alba). *Evolution* (2010) doi:10.1111/j.1558-5646.2010.00969.x.
71. Mátics, R., Hoffmann, G. & Owl, B. *Location of the transition zone of the Barn Owl subspecies Tyto alba alba and Tyto alba guttata (Strigiformes: Tytonidae)*. (2001).
72. Clements, J. F. *et al.* The eBird/Clements Checklist of Birds of the World: v2019. (2019).
73. Machado, A. P., Clément, L., Uva, V., Goudet, J. & Roulin, A. The Rocky Mountains as a dispersal barrier between barn owl (Tyto alba) populations in North America. *J. Biogeogr.* **45**, 1288–1300 (2018).

Tables

Table 1 - Population genetic diversity, inbreeding and divergence estimates for 11 populations of barn owls from the Western Palearctic. Standard deviations of the mean are provided between brackets for each parameter, see Methods section for details.

Pop	*N*	*#Pl*	*#PA*	*#Rare*	F_{IT}	F_{IS}	*Pop* F_{ST}
WC	9	2217235 (37007)	123016 (2465)	407403 (10568)	0.067 (0.054)	-0.022 (0.057)	0.116 (0.006)
PT	9	2639343 (22857)	102252 (2305)	539157 (10106)	-0.018 (0.042)	-0.008 (0.042)	0.003 (0.003)
FR	4	2151627 (0)	30290 (581)	287746 (1468)	0.039 (0.124)	0.043 (0.131)	0.050 (0.005)
CH	10	2494462 (10723)	47532 (730)	386654 (3117)	0.025 (0.019)	-0.011 (0.019)	0.036 (0.002)
DK	10	2410615 (15558)	40650 (1378)	349800 (5434)	0.026 (0.020)	-0.02 (0.021)	0.049 (0.002)
IT	9	2404069 (7267)	66297 (1638)	401842 (4483)	0.035 (0.012)	-0.022 (0.012)	0.052 (0.005)
SB	5	2336060 (0)	32096 (1515)	326906 (2519)	0.025 (0.011)	-0.038 (0.011)	0.056 (0.004)
GR	9	2454653 (7365)	44996 (1146)	378422 (4152)	0.018 (0.028)	-0.016 (0.027)	0.039 (0.002)
AE	10	2460422 (20650)	56260 (3439)	403259 (10465)	0.018 (0.060)	-0.001 (0.062)	0.030 (0.002)
CY	10	2338318 (48463)	113377 (2229)	480021 (13581)	0.022 (0.047)	-0.034 (0.049)	0.059 (0.004)
IS	9	2509099 (9500)	172624 (4018)	608944 (3597)	-0.019 (0.015)	-0.036 (0.016)	0.021 (0.003)

N: number of individuals in the population; #Pl: number of polymorphic sites per populations; #PA: number of private alleles per population; #Rare: Number of rare alleles per population; F_{IT}: mean individual inbreeding coefficient relative to the meta-population; F_{IS}: population level inbreeding coefficient; F_{ST}: population specific F_{ST} as in Weir and Goudet 2017. Populations: WC – Canary Islands, PT – Portugal, FR – France, CH – Switzerland, DK – Denmark, IT – Italy, SB – Serbia, GR – Greece, AE – Aegean Islands, CY – Cyprus, IS – Israel.

Figures

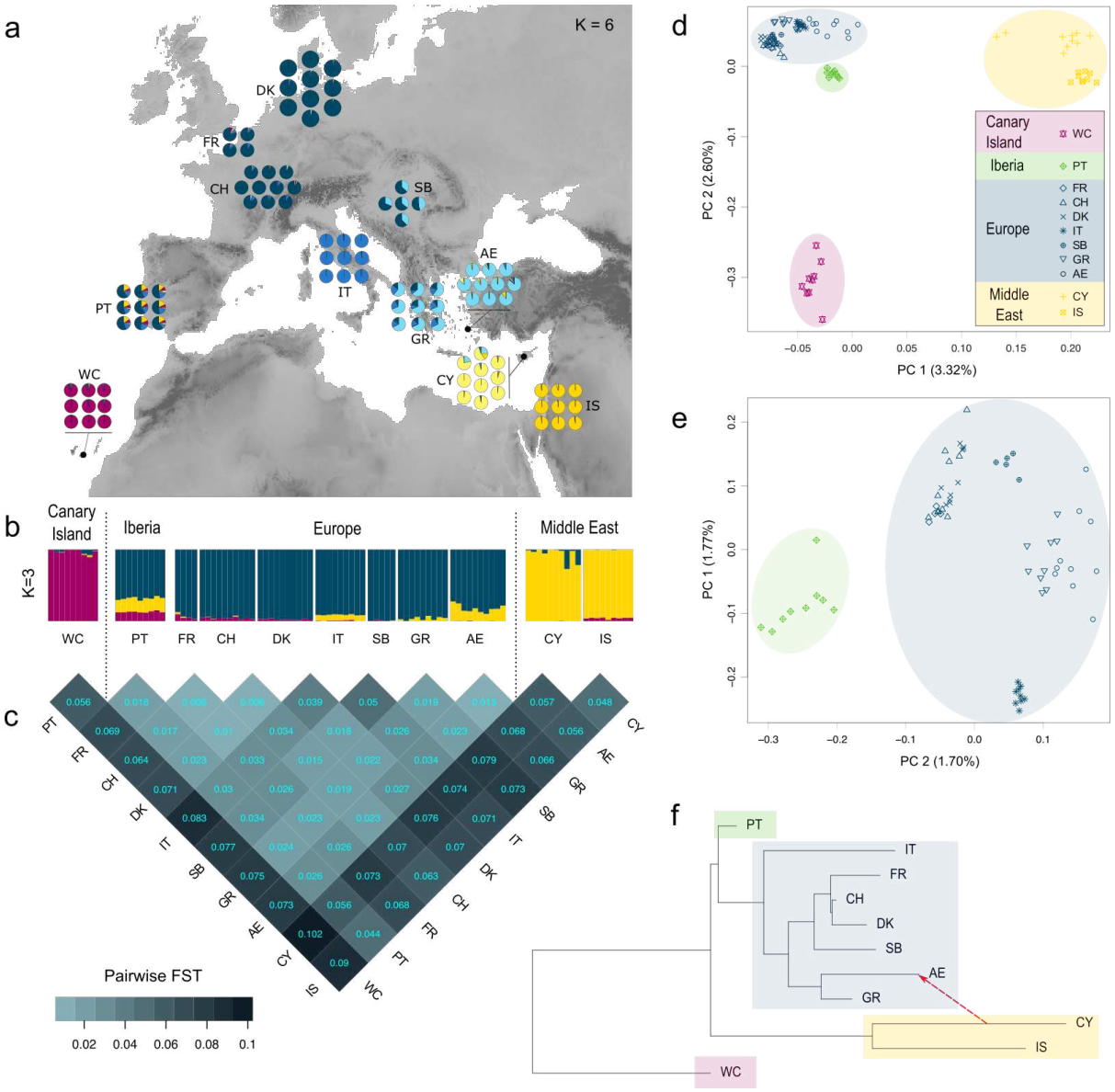

Figure 1 - Genetic structure of barn owl populations in Western Palearctic. (**a**) Population structure for K=6. Pie charts denote the individual proportion of each of lineages as determined by sNMF and are located at the approximate centroid of the sampled population. (**b**) Population structure for K=3. Each bar denotes the individual proportion of each of the 3 lineages as determined by sNMF. (**c**) Matrix of pairwise F_{ST} between barn owl populations in Western Palearctic. The heatmap provides a visual representation of the F_{ST} values given in each cell. (**d**) PCA based on full set of 94 individuals. Point shape denotes populations and colored circles enclose sample clusters observed in sNMF (K=3). Values in parentheses indicate the percentage of variance explained by each axis. (**e**) PCA based on of the 66 European individuals. (**f**) Population tree and the first migration event in Western Palearctic populations inferred by Treemix.

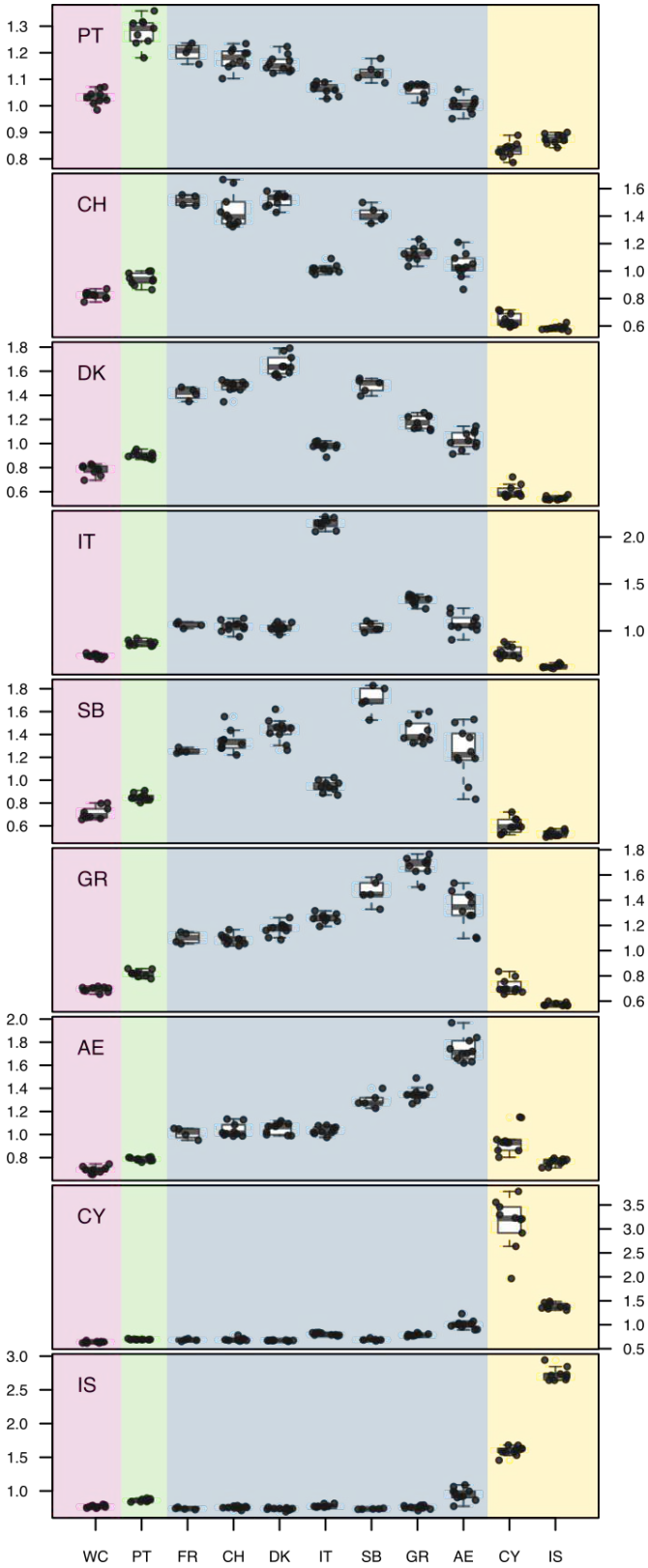

Figure 2 – Individual haplotype sharing between barn owl populations. Part of the total length of ChromoPainter chunks inherited from other genomes. Each graph summarizes the information of all the genomes from a given population, indicated on the top-left corner. Background colors match the lineages identified in fig. 1.

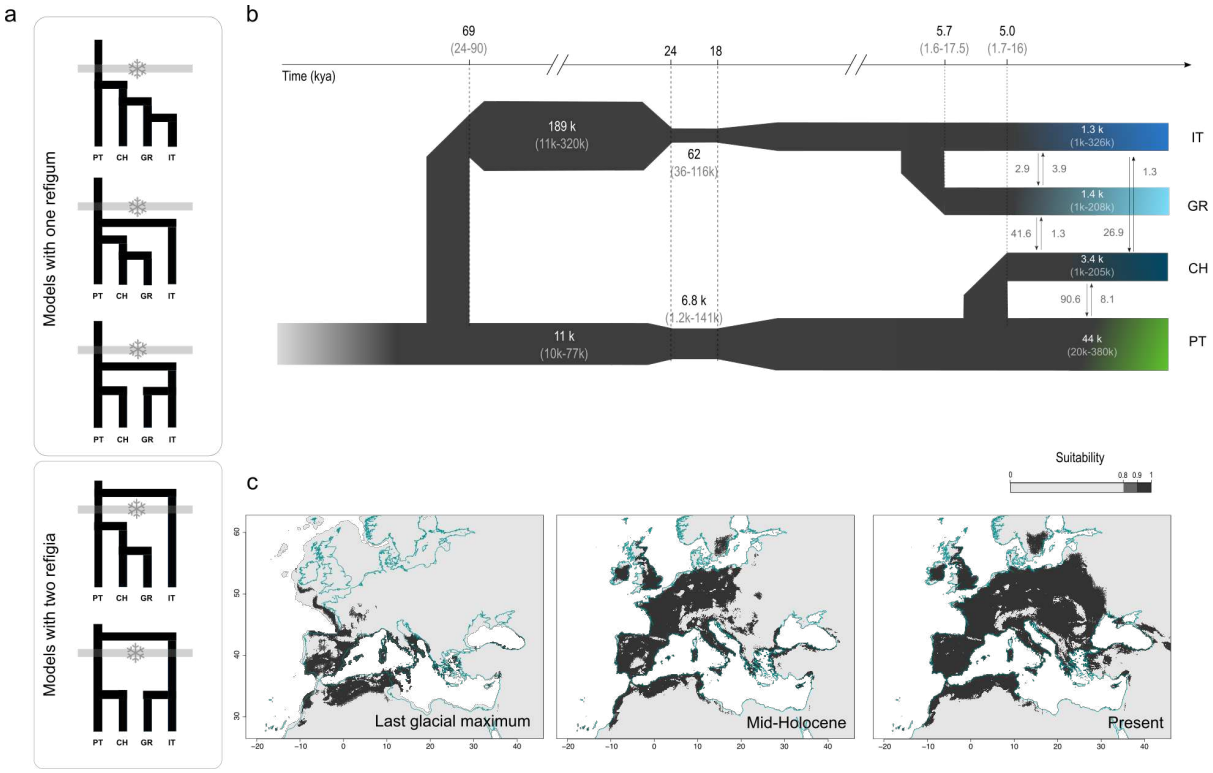

Figure 3 – Modeling of the history of the barn owl in Europe. (**a**) Schematic representation of the five demographic scenarios tested for the colonization of the Europe by barn owls. Three models included one refugium in the Iberia during the LGM while the last two included two refugia, one in Iberia and the second in Italy. Grey bars with snowflakes represent the last glaciation. (**b**) Best supported demographic model for the history of European barn owl populations as determined by fastsimcoal2. Time is indicated in thousands of years, determined using a 3-year generation time, confidence intervals at 95% are given between brackets. Population sizes (haploid) are shown inside each population bar; arrows indicate forward-in-time migration rate and direction. (**c**) Species distribution model of barn owls based on climatic variables, projected into the past (last glacial maximum (20 kya) mid-Holocene (6 kya)) and today's condition. Locations in dark grey were highly suitable in 90% of the models. Below that threshold cells were considered as unsuitable (lightest grey shade on the graph). The present coastline is outlined in blue in all graphs.

907

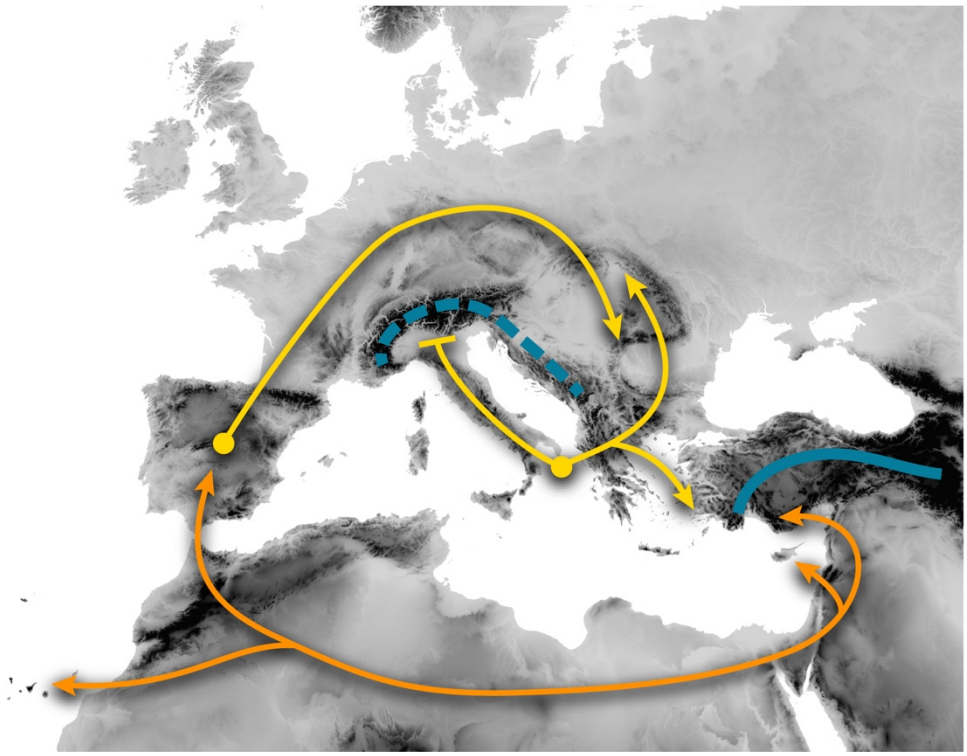

908
909

910 **Figure 4** – Schematic representation of the history of barn owls in the Western Palearctic
911 and the main barriers in the region. Orange arrows depict the colonization of the region by
912 the three main lineages (Levant, Canary Islands, European). Yellow arrows represent the
913 modeled postglacial recolonization scheme of Europe, with two distinct refugia (yellow
914 dots). Blue lines represent the main barriers identified in this work, namely the Alps in
915 Europe (dashed line) and the Taurus and Zagros mountains in Anatolia (solid line).